Mechanistic Study of Solvent-Dependent Formation of Extended and Stacked Supramolecular Polymers Composed of Bis(imidazolylporphyrinatozinc) Molecules

Akiharu Satake* [a][b], Yuki Suzuki[b], Motonobu Sugimoto[b], and Yusuke Kuramochi[a][b]

Abstract: Bis(imidazolylporphyrinatozinc) molecules linked via a 1,3-butadiynylene moiety respond to the solvents they are dissolved in to afford extended (E) or stacked (S) supramolecular polymers exclusively. This system is expected to be a solvation/desolvation indicator. However, the principle of the solvent-dependent formation and the mechanism of the transformation between E- and S-polymers is unclear. Formation of the polymers was considered to depend on the two types of complementary coordination bonds and π–π interaction among the porphyrins. In this study, the contribution and the solvent dependence of both the coordination bonds and the π–π interaction were investigated. The results indicated that the coordination terms are clearly weakly or little solvent dependent. However, π–π interaction works effectively only in the inside porphyrins in an S-polymer and is strongly solvent dependent. Thermodynamic analysis revealed that the formation of E- or S-polymers in solutions is determined by total energies and the type of solvent used. The process of transformation from E- to S-polymer was determined by gel permeation chromatography. The kinetics of the transformation were also determined. The role of the terminal imidazolylporphyrinatozinc moieties was also investigated. Transformation from E- to S-polymer occurs via an exchange mechanism among the polymers, induced by attack on the terminal moieties of the polymers.

Introduction

Stimuli-responsive structural changes of molecules[1] and supramolecules[2] are useful in molecular-based applications, such as molecular switch[3], chemical sensor[4], drug delivery[2a], and programmed molecular architecture[5]. Structural changes are often accompanied by changes in photo-electronic and/or physical properties, such as absorption[4a], emission[4b, 6], circular dichromism spectra[7], viscosity[2b], and gel formation[2c]. In such cases, the materials are potential sensors or indicators, able to detect circumstances, followed by translating them to other signals.

[a] Prof. A. Satake, Mr. Y. Suzuki, Mr. M. Sugimoto, Dr. Y. Kuramochi
Graduate School of Science
Tokyo University of Science
1-3 Kagurazaka, Shinjuku-ku, Tokyo 162-8601, Japan
E-mail: satake@rs.kagu.tus.ac.jp
[b] Prof. A. Satake, Dr. Y. Kuramochi
Department of Chemistry, Faculty of Science Division II,
Tokyo University of Science

Supporting information for this article is given via a link at the end of the document.

In the field of supramolecular analytical chemistry[2a], increasing the selectivity and sensitivity of target molecules remains challenging, especially in the presence of similar and competitive molecules. Another challenging task in the field is the detection of weak interactions, such as van der Waals interactions, in the presence of various potentially stronger interactions, such as hydrogen bonding and coordination bonding. The term, van der Waals interaction, is a generic name given to describe inter- and intramolecular weak interactions that work mainly among neutral nonpolar compounds in solutions and crystals[8] and, supplementary, with other strong interactions, such as hydrogen and coordination bondings, especially in biological recognition[9]. However, fully understanding weak interactions would involve understanding Nature. A deeper understanding of weak interactions is desirable, but it is difficult to understand them alone, separately from strong interactions, because they usually tend to be obscured by other stronger interactions.

In an analogy in the field of physics, a small gravitational wave was recently observed in the presence of various noises on Earth by using well-designed apparatus[10]—this won the 2017 Nobel Prize for Physics[11]. In the field of chemistry, the double-mutant cycle analysis[12] has been adopted to eliminate other effects from wild signals. By using the double-mutant cycle analysis, it is possible to estimate the strengths of weak hydrogen bonding[13], and dispersion interaction between alkyl groups[14], or alkyl and aromatic[15] groups. Another strategy to detect weak interactions involves using polymeric systems that have multi-interaction sites[4d]. When each interaction site is associated with another, with a positive allosteric effect[16], the weak interactions are amplified through the whole structural change of the polymer[4d, 17].

Recently, we successfully developed a stimuli-responsive supramolecular polymer system to detect weak van der Waals interactions between solvents and neutral nonpolar zinc porphyrin[18]. In this system, interconversion of supramolecular polymers composed of bis(imidazolylporphyrinatozinc) molecules linked via a 1,3-butadiyne moiety, **1Zn$_2$** and **2Zn$_2$**, occurred, depending on the solvents used. For example, they gave extended (E-) polymer in “good” solvents, such as chloroform ($CHCl_3$), whereas they gave stacked (S-) polymer in “poor” solvents, such as 1,2-dimethoxyethane (DME), as shown in Figure 1. The UV–vis absorption spectra of E- and S-polymers differ significantly and the interconversion apparently seems to be a two-state change, therefore one can easily know whether the tested solvent was “good” or “poor” (just like in a litmus test). In this study, we used this system to investigate 67 types of solvents and liquids.

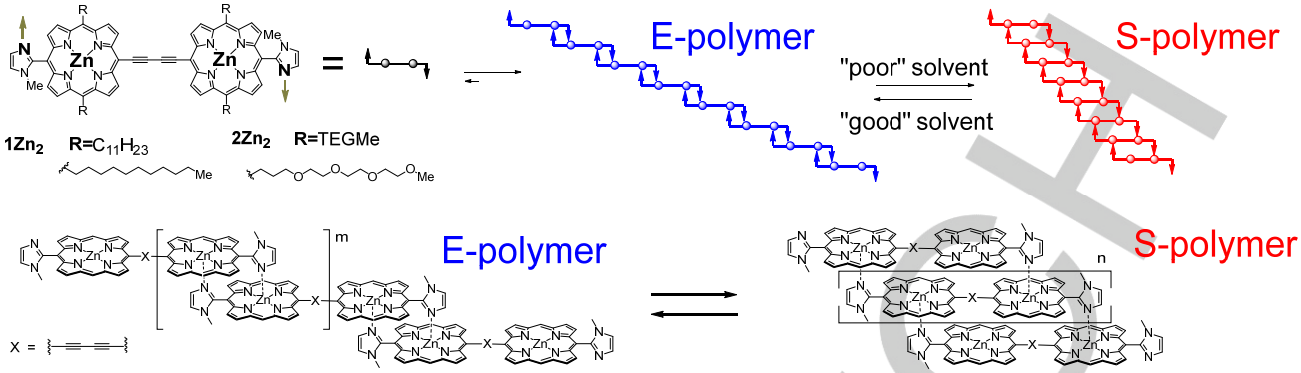

Figure 1. Structures of bis(imidazolylporphyrinatozinc) **1Zn$_2$** and **2Zn$_2$**, and their coordination-organized polymers, extended (E-) and stacked (S-) polymers. Symbolic images of them are also illustrated, in which arrows indicate imidazole moieties and their coordinating directions, and circles symbolize zinc ions in zinc porphyrins. Blue and red colors symbolize E- and S-polymers, respectively.

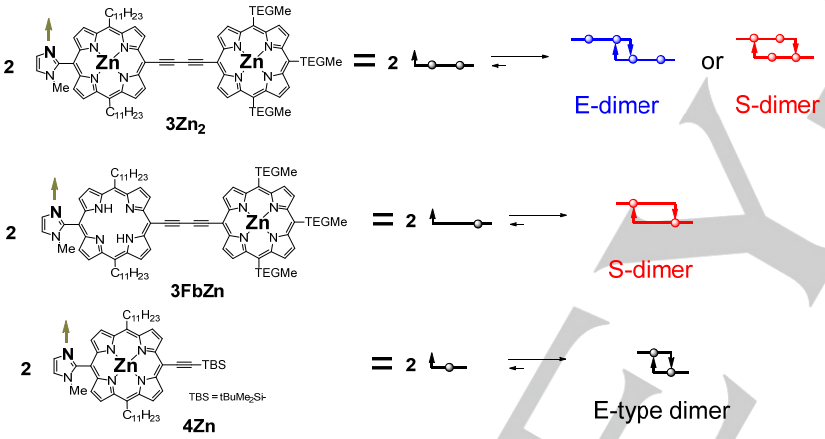

Figure 2. Structures of monoimidazolylporphyrin derivatives **3Zn$_2$**, **3FbZn**, and **4Zn**, and their symbols. They form self-assembled dimers by complementary coordination. Biszinc porphyrin **3Zn$_2$** has the potential to form both extended (E-) and stacked (S-) dimers, whereas monozinc porphyrin **3FbZn** and **4Zn** give only S-dimer and E-type dimer, respectively.

The formation of E- and S-polymers depends mainly on E- or S-types of complementary coordination bonds and π–π interaction among porphyrins. If the contributions of the coordination bonds and the π–π interactions can be considered separately then the principle of the dynamic system becomes clearer. Furthermore, to understand the mechanism of the transformation between E- and S-polymers, it is important to use the system as a solvation/desolvation indicator. Separating the contributions, we now study the effect of solvents on E- and S-types of complementary coordination bonds in dimer systems, as shown in Figure 2. In the dimer systems, π–π interactions among the porphyrins are much smaller, or even negligible, compared with those in long polymeric systems (see Figure 1). This is because no porphyrin moiety exists that covers both the top and the bottom in the S-dimer, whereas most of the porphyrins cover both sides in the long S-polymer (inside porphyrins in S-polymer). On the other hand, rotational freedom per porphyrin unit occurs in E-dimer and E-polymer.

We, therefore, determined the contribution of the coordination strength of the E- and S-type coordination from the dimer systems. We separated the contribution of the coordination strength from the π–π interactions in the polymer systems. We examined **3Zn$_2$**, **3FbZn**, and **4Zn** (Figure 2). **3Zn$_2$** has the potential to form both E- and S-dimers, and their solvent dependency can be determined. **3FbZn** and **4Zn** give only S-dimer and E-type dimer, respectively.

In this paper, we also examined E-/S-compositions and lengths of supramolecular polymers of **1Zn$_2$**, associated with solvent compositions, using gel permeation chromatography (GPC). Although E-polymers are very large polymers, they can be dissolved in chloroform. Thus, a chloroform solution of E-polymers could be injected into a GPC column, then its reconstitution and transformation into S-polymer carried out in a mixture of chloroform and DME as eluent. The flow rate used was sufficiently slow to realize this reconstitution and transformation. The observed compositions and lengths of supramolecular polymers are considered to be thermodynamically controlled products under the solvent compositions we used as eluent. To determine the effect of the terminal imidazolyl zinc porphyrin moieties, E-polymers of **1Zn$_2$**

end-capped by **4Zn** were also investigated. We also determined the kinetics of the transformation from E- to S-polymers. Temperature-jump experiments, using samples of different concentrations, gave the order of the transformation as well as insight into the mechanism.

In this paper, we discuss the principle and mechanism of solvent-dependent formation of E- or S-polymers as well as transformation from E- to S-polymers composed of **1Zn₂** or **2Zn₂**, based on all our experimental results.

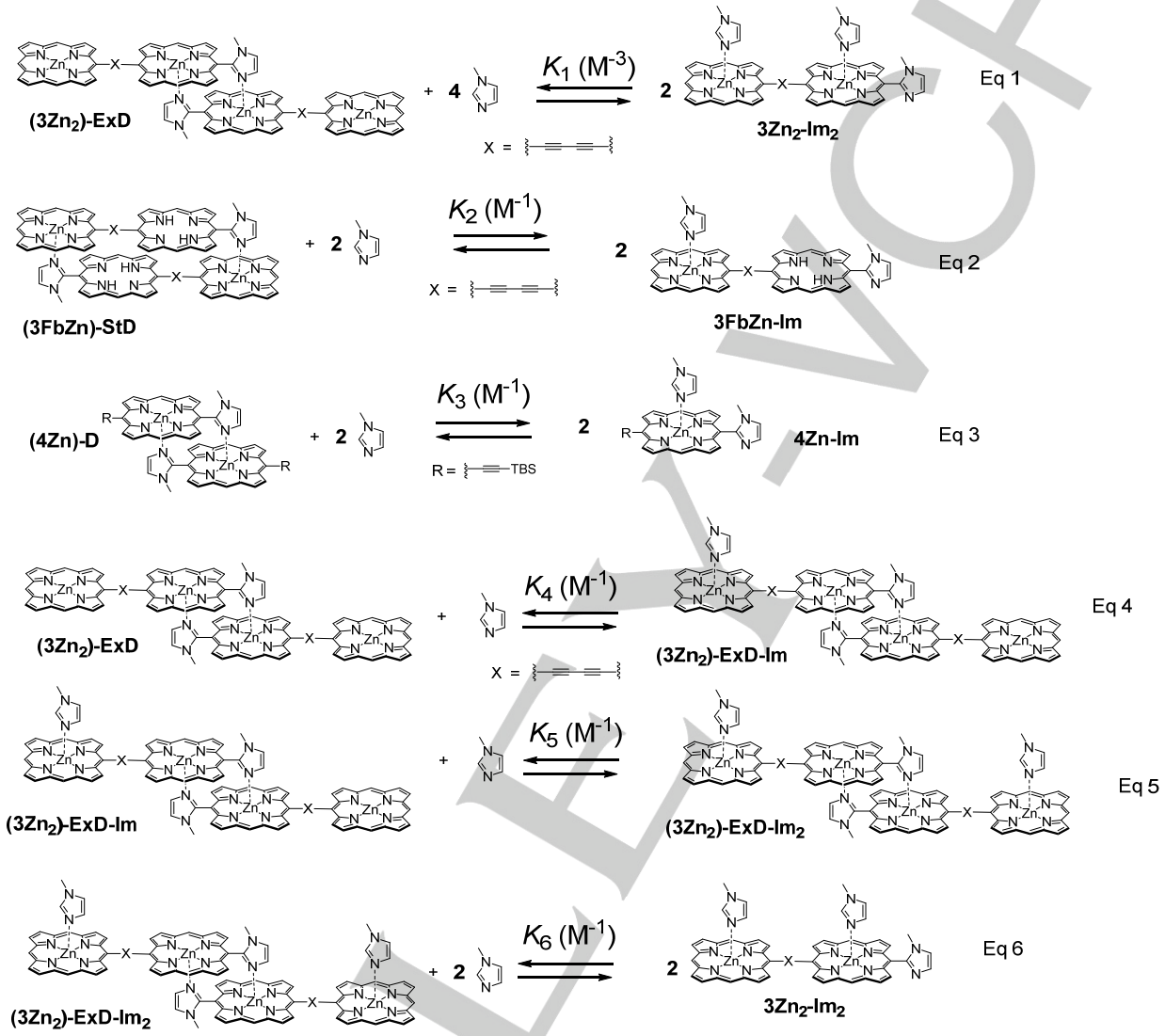

Figure 3. Coordination equilibria among zinc porphyrins, **3Zn₂**, **3FbZn**, and **4Zn**, and *N*-methylimidazole.

Results

Formation of self-assembled dimer of 3Zn₂ in various solvents

3Zn₂ was dissolved in various solvents (acetone, DME, toluene, and chloroform) to give solutions of approximately 6×10^{-7} M. The UV–vis spectra are shown in Figure S1. **3Zn₂** compounds are considered to be able to give two types of complementary coordination dimers, E- and S-dimers, as shown in Figures 2 and S2. The structures formed in the various solvents were determined by comparing their spectra with the UV–vis spectra of **3Zn₂** and **3FbZn** in chloroform. **3Zn₂** and **3FbZn** gave E- and S-dimers in chloroform, respectively, as confirmed by ^{1}H NMR spectral analyses[18]. In the UV–vis spectra, the characteristic peaks used to identify the E- and S-dimers appear around 720 and 745 nm, respectively (Figure S3). Since this difference is sufficiently large (25 nm) and the respective peaks have characteristic shapes, the S-dimer (if present) is easily detected. The UV–vis spectral shapes and peaks in Figure S1 indicate that **3Zn₂** gave E-dimer in all four solvents. **1Zn₂** gave S-polymer in the solvents acetone, DME, and toluene, but not chloroform.

Determination of dissociation constants in various solvent systems by UV–vis spectroscopy

To determine the interaction strengths of imidazole-appended zinc porphyrin dimers, the competitive dissociation experiments of **3Zn$_2$**, **3FbZn**, and **4Zn** with *N*-methylimidazole (Im) were carried out as shown in Eq 1–6 in the four solvents (acetone, DME, toluene, and chloroform). As a reference, UV–vis titration experiments of tetraphenylporphyrinatozinc (ZnTPP) with Im were also carried out in various solvents and solvent systems. The association constants K_{S1} of ZnTPP and Im are defined as in Eq S1 (SI), and the values obtained in various solvents and solvent systems are tabulated in Table S1. As shown in Figure 3, the dissociation process of the extended dimer of **3Zn$_2$** without Im (**(3Zn$_2$)-ExD**) to form monomeric **3Zn$_2$-Im$_2$** coordinated by two Im molecules (see Eq 1, also includes Eq 4–6). To compare the dissociation constants among **3Zn$_2$**, **3FbZn**, and **4Zn**, the dissociation constants K_6, K_2, and K_3 are tabulated in Table 1.

Table 1. Competitive dissociation constants K_6, K_2, and K_3 at 298 K.

Solv.	**(3Zn$_2$)-ExD-Im$_2$** K_6/ M^{-1} [a]	**(3FbZn)-StD** K_2 / M^{-1}[b]	**(4Zn)-D** K_3 / M^{-1}[b]
acetone	2.5×10^{-3}	6.0×10^{-3}	5.0×10^{-3}
DME	6.5×10^{-3}	8.5×10^{-2}	7.5×10^{-3}
$CHCl_3$	5.0×10^{-3}	6.0×10^{-2}	6.0×10^{-3}
toluene	6.5×10^{-3}	3.5×10^{-1}	2.5×10^{-2}

[a] Curve fitting analysis to estimate K_6 was performed by assuming $K_4 \approx K_5 \approx K_{S1}$, which were consistent with the experimental data. [b] K_2 and K_3 values were directly determined by titration experiments with *N*-methylimidazole.

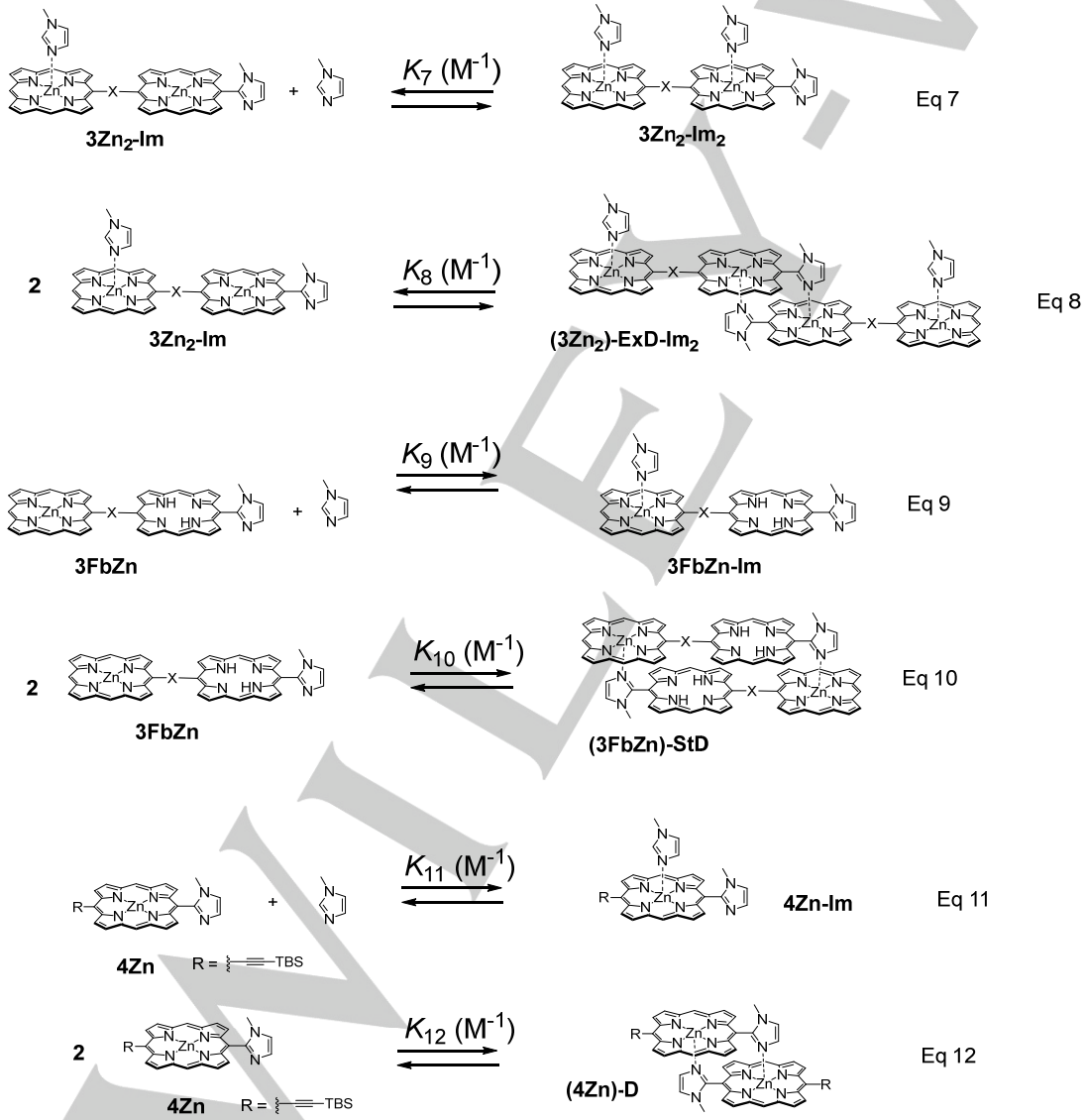

Figure 4. Coordination equilibria among zinc porphyrins, **3Zn$_2$**, **3FbZn**, and **4Zn**, and *N*-methylimidazole.

Table 2. Self-association constants K_8, K_{10}, and K_{12} and the Gibbs free energy changes at 298 K.

Solv.	**3Zn$_2$-Im** K_8/ M^{-1} [a]	ΔG^0_{298} / kJ/mol	**3FbZn** K_{10} / M^{-1}[a]	ΔG^0_{298} / kJ/mol	**(S-E) dimer** $\Delta\Delta G^0_{298}$ / kJ/mol	**4Zn** K_{12} / M^{-1}[a]	ΔG_{298} / kJ/mol
acetone	4.0×10^{10}	–61	1.7×10^{10}	–58	3	2.0×10^{10}	–59
DME	5.0×10^{8}	–50	3.8×10^{7}	–43	7	4.8×10^{8}	–49
$CHCl_3$	4.4×10^{9}	–55	2.9×10^{7}	–48	7	2.9×10^{9}	–54
toluene	4.4×10^{11}	–66	8.2×10^{9}	–57	9	1.2×10^{11}	–63

[a] Self-association constants K_8, K_{10}, and K_{12} can be calculated by $K_8 = (K_7)^2/K_6$, $K_{10} = (K_9)^2/K_2$, and $K_{12} = (K_{11})^2/K_3$, assuming $K_7 \approx K_9 \approx K_{11} \approx K_{S1}$….

Determination of self-association constants in various solvent systems

The self-association constants of **3Zn$_2$-Im**, **3FbZn**, and **4Zn** (defined as in Eq 8, 10, and 12 in Figure 4) can be calculated as follows: $K_8 = (K_7)^2/K_6$, $K_{10} = (K_9)^2/K_2$, $K_{12} = (K_{11})^2/K_3$. Because K_7, K_9, and K_{11} in Eq 7, 9, and 11, respectively (see Figure 4), cannot be determined experimentally, we made the assumption that they were nearly equal to K_{S1} in the same solvents. Therefore, $K_8 \approx (K_{S1})^2/K_6$; $K_{10} \approx (K_{S1})^2/K_2$; $K_{12} \approx (K_{S1})^2/K_3$. Here, K_6, K_2, and K_3 were determined experimentally as the dissociation constants (see Table 1). We also applied the K_{S1} values to K_4 and K_5 in the same solvents to determine K_6. The obtained self-association constants, K_8, K_{10}, and K_{12}, are tabulated in Table 2, together with their Gibbs free energy changes (ΔG^0) at 298 K. Differences between the ΔG^0 of E-dimer of **3Zn$_2$-Im** and ΔG^0 of S-dimer of **3FbZn**, namely $\Delta\Delta G^0$, are also given. Although the energy difference between the E-dimers and S-dimers of **3Zn$_2$**, **3Zn$_2$-ExD**, and **3Zn$_2$-StD** (Figure S2) could not be determined (the S-dimer was not observed), the energy difference between the dimers of **3Zn$_2$-Im** and **3FbZn** can be estimated as $\Delta\Delta G^0_{298}$, as shown in Table 2. Differences are in the range 3–9 kJ/mol in the four solvents, suggesting that the energy difference between the E-dimer and S-dimer of **3Zn$_2$** is small. Although the latter is small, it is evident that the E-dimer is always more stable than the S-dimer, irrespective of the solvent used. The $\Delta\Delta G^0_{298}$ values are obtained from the virtual equilibrium between **3Zn$_2$-Im** (E-dimer) and **3FbZn** (S-dimer) (Figure S35). In the real equilibrium between the E- and S-dimers of **3Zn$_2$**, the $\Delta\Delta G^0_{298}$ values may be larger than those in the virtual, because the S-dimer was scarcely observed. In case of ΔG^0_{298} = 10 kJ/mol, the equilibrium constant K corresponds to 0.0177, from the equation $\Delta G^0 = -RT\ln K$ (R: the gas constant), in which the major component is 98.3%. From the UV–vis spectra in Figure S1, it is difficult to detect the presence of less than a very low percentage of minor S-dimer. The difference between the $\Delta\Delta G^0_{298}$ values, between the virtual and real equilibria, is considered to be insignificant. Hence, the $\Delta\Delta G^0_{298}$ in the real equilibrium is estimated to be in the order of between 10 and a dozen kJ/mol.

Solvent-dependent structural changes were not observed in the dimer systems of **3Zn$_2$**, in which the E-dimer is always more stable, irrespective of the solvent used. The polymer systems of **1Zn$_2$** and **2Zn$_2$** were then investigated.

GPC analysis of supramolecular polymers

Figures 5 and S22 show GPC charts of **1Zn$_2$** and **2Zn$_2$**, respectively, monitored at 500 nm. The following solvent mixtures were used as eluents: $CHCl_3$:DME = 100:0, 90:10, 80:20, and 70:30. At the monitoring wavelength, both E- and S-polymers are expected to be detected to the same extent because the wavelength is one of the isosbestic points in the equilibrium between E- and S-polymers. Similar amounts of **1Zn$_2$** and **2Zn$_2$** were injected for each GPC run, hence the total area of the chromatogram in each run should be almost constant if all the components are eluted. Assignment of structures as E- or S-polymer at each retention time (RT) could be performed from the UV–vis absorption spectra. In the figures, only the peaks marked with asterisks were S-polymers; all others were E-polymers. In GPC, larger polymers tend to elute as earlier RT components. The exclusion limit of this column was about 3.5–4.5 min, slightly depending on the solvent conditions. The mass scale, prepared from calibration plots, is shown at the top of the figures. It is noted that the mass scales of the polymers are distributed over a wide range as $\log_{10}$ 9–$\log_{10}$ 4 Da; no monomers, dimers, and small oligomers were observed. Therefore, only relative size changes among long polymers (from the GPC charts) are discussed.

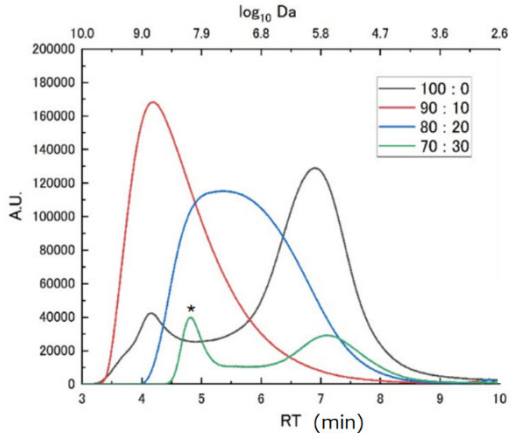

Figure 5. Solvent effect on GPC charts of **1Zn₂** by using $CHCl_3$:DME = (black) 100:0, (cyan) 90:10, (red) 80:20, (green) 70:30 as the eluent. Monitored at 500 nm on a PLgel 20 μm mixed-A column (Polymer laboratories, exclusion limit 40,000 kDa). 10 μL of 6.0×10^{-4} M chloroform solutions were injected. The asterisk peaks were assigned as S-polymer on the green chart, and all other components were assigned as E-polymers on any line.

The chromatogram of **1Zn₂** (Figure 5) shows a peak maximum at about RT 7.0 min when only chloroform is used as the eluent. The UV–vis absorption spectra indicate that all the structures were E-polymers. When a mixture of $CHCl_3$:DME = 90:10 is used as an eluent, the peak maximum was observed at ca RT 4.0 min (reaching the exclusion limit), indicating the formation of much longer polymers compared with those formed in 100% $CHCl_3$. In the case of $CHCl_3$:DME = 80:20, the elution curve became broad, and it was observed in the later RT range, indicating that the lengths became shorter than those formed in $CHCl_3$:DME = 90:10. Further increasing the ratio of DME to $CHCl_3$ to 70:30 resulted in the following: a peak of S-polymer was observed at 4.8 min (perhaps reaching the exclusion limit) and E-polymers eluted around 7.2 min. At this ratio of $CHCl_3$:DME (70:30), transformation of E- to S-polymers of **1Zn₂** occurred. The total area of the elution curve obtained here decreased significantly compared with that in the other cases (for other solvent ratios). Here, we considered the following phenomenon to apply: S-polymers elute from a GPC column with difficulty because they tend to be aggregated and entangled by themselves, as has previously been observed in an atomic force microscopy image[18]. In our series of experiments, the following took place when we increased the DME content in the $CHCl_3$:DME solvent mixture: the relatively shorter E-polymers first became longer (from 100:0 to 90:10), then they became shorter again (at 80:20), and at 70:30 they were partly transformed to S-polymers.

A similar trend was observed in the chromatograms of **2Zn₂** in Figure S22. Relatively shorter E-polymers were observed in $CHCl_3$:DME = 100:0, then their lengths increased, reaching the exclusion limit in $CHCl_3$:DME = 90:10. They then became increasingly shorter when the ratios of DME were increased (80:20 and 70:30). Transformation of E- to S-polymers occurred in $CHCl_3$:DME = 60:40 in the case of **2Zn₂** (Figure S23). The slight difference in the $CHCl_3$:DME ratio at which the transformation to S-polymers between **1Zn₂** and **2Zn₂** takes place is due to a difference in the substituents on **1Zn₂** and **2Zn₂**. The latter has more hydrophilic triethyleneglycol derivatives, rather than undecyl groups, hence the timing of the transformation to S-polymer takes place was shifted to a higher DME content in **2Zn₂**. Contour maps, recorded using GPC with photodiode array (PDA) detection, are shown in Figure S24. We can compare the UV–vis spectra of the eluted samples continuously. It is noted that UV–vis spectra of E-polymer were identical under any eluent conditions and at any elution time. Similarly, the UV–vis spectra of S-polymer were also identical at any elution time. These results indicate that the UV–vis spectra of E- and S-polymers do not depend on their polymer lengths in the observed ranges.

E-polymers of **1Zn₂** have active imidazolylporphyrinatozinc moieties at the terminal ends. To examine the effects of the terminal ends, monoimidazolyporphyrinatozinc **4Zn** was mixed with **1Zn₂**. We expected that the **1Zn₂** terminals would be capped by heterogeneous complementary coordination bonds between **1Zn₂** and **4Zn**. Mixtures of **1Zn₂** and **4Zn** (100:0, 50:1, 10:1, 5:1, 2:1, and 1:1) were analyzed under the same GPC conditions, using mixtures of $CHCl_3$:DME = 90:10, 80:20, 70:30, and 60:40 as eluents. All the GPC charts are shown in Figures S25, 6, and S26. These GPC charts include the same eluents as in Figures 6 and S26 and the same ratios of **1Zn₂** and **4Zn** as in Figure S25. In each experiment, the same amounts of **1Zn₂** were injected to the GPC column but those of **4Zn** varied. A homodimer of **4Zn** shows very low absorbance (AU <20 000) at the monitoring wavelength (500 nm) at RT 9.4 min, as seen in Figures S27 and S28. Therefore, visible elution curves observed in Figures S25, 6, and S26 are derived from only **1Zn₂** and/or heterocomposites of **1Zn₂** and **4Zn**, not from homodimer of **4Zn**. In these figures, peaks marked with asterisks are assigned as S-polymers. The contour maps, recorded using a combination of PDA and GPC, are shown in Figures S29–S32.

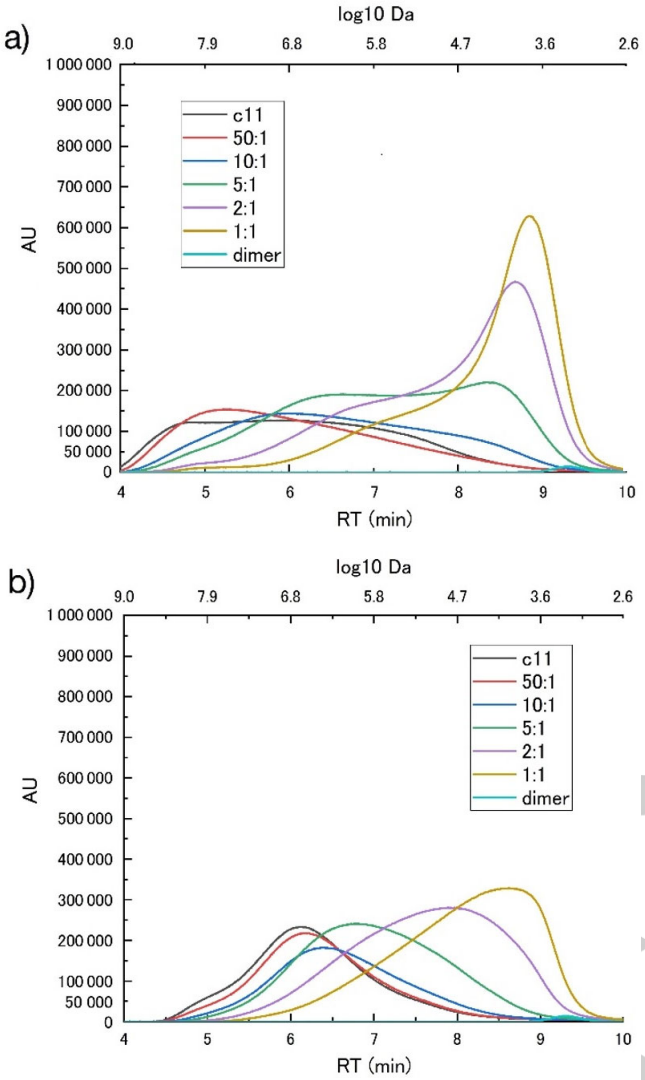

Figure 6. Effect of molar ratio of **4Zn** on GPC charts of mixtures of **1Zn$_2$** and **4Zn** in $CHCl_3$:DME = (a) 90:10 and (b) 80:20 as the eluent. These charts are prepared from the same data used in Figure S25. Asterisk peaks indicate S-polymers. Ratios of **1Zn$_2$** and **4Zn** = (black) 100:0, (red) 50:1, (cyan) 10:1, (green) 5:1, (purple) 2:1, (brown) 1:1 and (sky blue) only **4Zn** (RT 9.4 min, AU <20 000).

Under the eluent condition of $CHCl_3$:DME = 90:10, components around RT 7 min were decreased by mixing with **4Zn** (**1Zn$_2$**:**4Zn** = 50:1, compared with 100:0), whereas components around RT 5 min were increased. (Figures S25a and S25b, Figure 6a). These results can be explained by certain amounts of **4Zn** that capped the terminals of E-polymers and affected the equilibria among the E-polymers. When the ratios of **4Zn** to **1Zn$_2$** were increased as follows: 10:1, 5:1, 2:1, and 1:1 (Figures S25c–f), the lengths of E-polymers were decreased. Interestingly, their distributions appear to be polydispersed. These results indicate that **1Zn$_2$** and **4Zn** were not effectively mixed. Possible coordination equilibria among zinc porphyrins, **1Zn$_2$** and **4Zn**, are shown in Figure 7. The result suggests that K_{13} and/or K_{14} is larger than K_{15} in Eq 13, 14, and 15 (Figure 7).

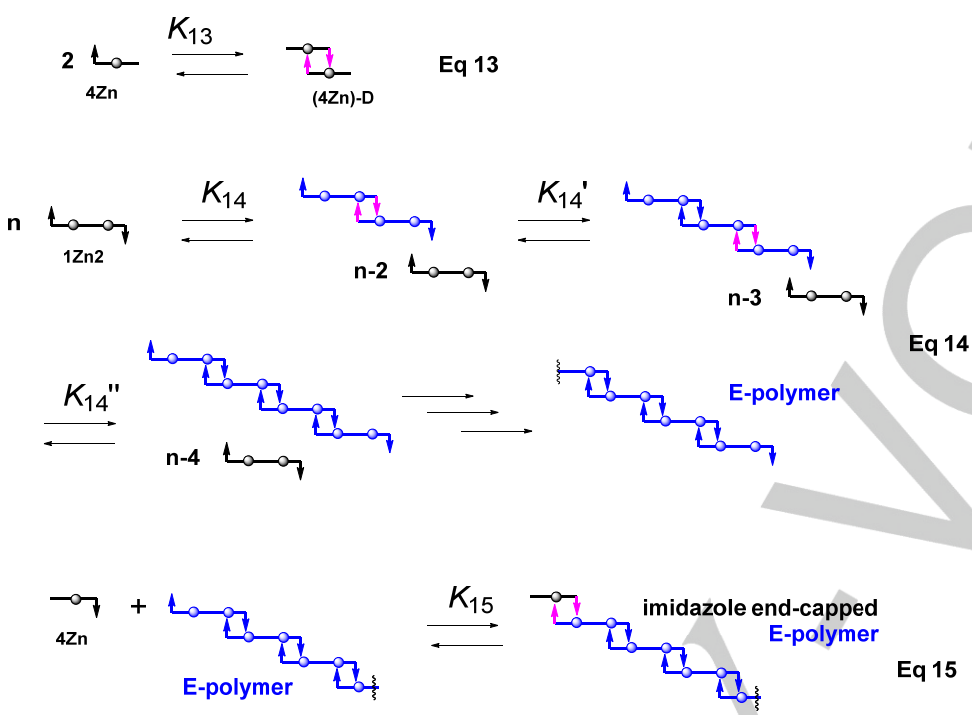

Figure 7. Coordination equilibria among zinc porphyrins, **1Zn₂** and **4Zn**.

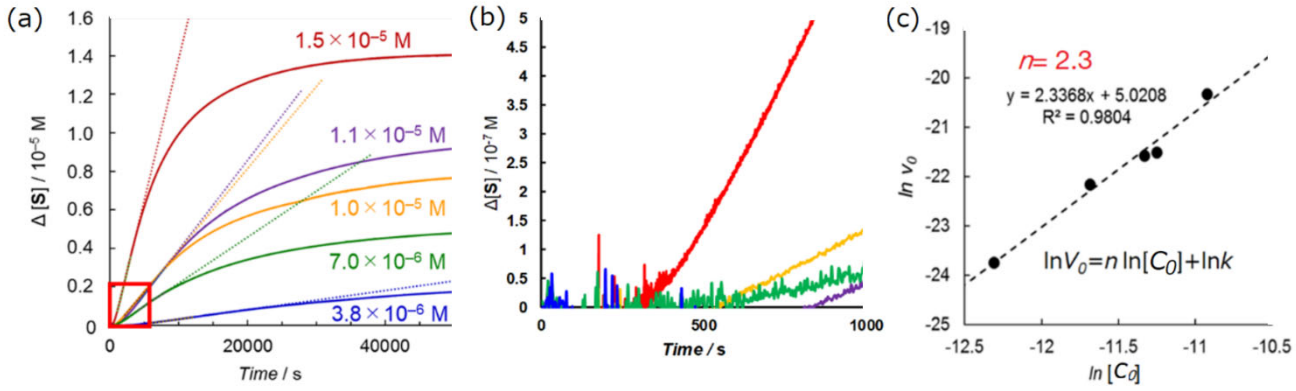

Figure 8. (a) Concentration-dependent time-courses of E to S transformation in temperature jump experiments (from 343 K to 293 K) as shown in Figure 14: from the top to bottom 15, 11, 10, 7.0, and 3.8 x 10^{-6} M, (b) enlargement of the red square in (a), (c) relationship between logarithm of the initial concentrations c_0 and logarithm of the initial transformation rates v_0.

Regarding the eluent condition of $CHCl_3$:DME = 80:20 (Figure 6b), increasing ratios of **4Zn** to **1Zn₂** also yielded shorter E-polymers. This is in contrast to the eluent condition of $CHCl_3$:DME = 90:10. Distributions in the case of $CHCl_3$:DME = 80:20 were close to monodispersed. This result suggests that K_{15} becomes comparable to K_{13} and K_{14}, and heterocomposites of **1Zn₂** and **4Zn** are generated (see Eq 15).

When the ratio of DME in the eluents was further increased to $CHCl_3$:DME = 70:30 and 60:40, formation of S-polymers was observed at about RT 5.0–5.2 min (Figure S26). The total areas of the elution curves varied among samples of **1Zn₂**:**4Zn** = 100:0, 50:1, 10:1, 5:1, 2:1, and 1:1. A decrease in the total area probably corresponds to the formation of S-polymers, which elute with difficulty from the GPC column. In the cases of samples containing significant amounts of **4Zn**, such as

1Zn$_2$:**4Zn** = 5:1, 2:1, and 1:1, there seems to be no decrease in the total area. These results indicate that transformation of E- to S-polymers is suppressed by the end-capping with **4Zn**, affording short E-polymers that have a low **1Zn$_2$**/**4Zn** ratio. On the basis of the mass scale shown at the top of Figure S26d, the peaks observed at RT 8.5 (**1Zn$_2$**:**4Zn** = 5:1), 8.7 (2:1), and 8.9 (1:1) min correspond to end-capping oligomers that have the **1Zn$_2$**/**4Zn** ratios 16.5, 6.0, and 4.0, respectively.

Temperature-jump experiments

The concentration dependence of the kinetics in the transformation from E- to S-polymers was determined by temperature-jump experiments. A balance point, where E- and S-polymers of **2Zn$_2$** exist comparably, was prepared in a binary solvent system of 1,1,2,2-tetrachloroethane (TCE) and DME (6:4). Under dilute conditions of the solvent system, E- and S-polymers of **2Zn$_2$** are apparently in equilibrium. Thermodynamic parameters of the equilibrium have been studied by variable temperature UV–vis spectral experiments[18]. The ΔH = –29.2 kJ/mol and ΔS = –90.8 J K/mol were determined for the transformation from E- to S-polymers, indicating that it was driven by enthalpy.

In the binary solvent system, the temperature was increased to 343 K to shift the equilibrium to the E-polymer. Thereafter, the temperature was set at 293 K. The progress of the transformation of E- to S-polymers was monitored at 768 nm on a UV–vis spectrometer. Concentration-dependent time courses of the transformation are shown in Figure 8a; the initial stages are enlarged in Figure 8b. The transformations occurred after an induction period of about 500 s. The relationship between the logarithm of the initial concentrations c_0 and the logarithm of the initial rates of the transformations without the induction periods are plotted in Figure 8c. A good linear relationship was observed in Figure 8c. From the slope, the order of the transformation was determined as 2.3. This result indicated that more than two molecules or aggregates are associated with one another in the transformation. The existence of the induction periods suggested the formation of nuclei of S-polymers at the initial stage. This working hypothesis was supported by shortening the induction period, followed by acceleration of the transformation, when nuclei of S-polymers were added to a solution at the initial stage. Such a nucleation and elongation mechanism is frequently observed in various supramolecular polymer systems[19], [20].

Discussion

Solvent effect on the coordination bond between tetraphenylporphyrinatozinc (ZnTPP) and *N*-methylimidazole (Im)

To discuss the solvent effect on the coordination between zinc porphyrin and Im, the association constants of ZnTPP and Im were determined in four solvents, acetone, DME, toluene, and chloroform, as well as in mixtures of $CHCl_3$ and DME (Table S1). The $CHCl_3$/DME mixtures were used as eluents in the GPC analyses. Among the pure solvents, the association constants decreased in the order toluene, acetone, $CHCl_3$, and DME. When DME was added to $CHCl_3$ to prepare the solvent mixtures, the association constants decreased gradually and became close to that in DME alone.

In general, Gutmann donor numbers (*DN*) are known to be related to coordination abilities to Lewis acids[21]. However, the numbers, toluene (*DN* 0.1), acetone (*DN* 17), chloroform (*DN* 4), and DME (*DN* 20)[21], do not seem to apply to the ZnTPP-Im system. The discordance probably arises because the *DN*s were measured for antimony pentachloride ($SbCl_5$), which is a relatively strong and hard Lewis acid, unaffected by steric hindrance. Coordination bonds on zinc porphyrin are affected by steric hindrance[22], and the Lewis acidity is moderate. In our previous study of **1Zn$_2$** and **2Zn$_2$**[18], only $CHCl_3$ gave the E-polymer, whereas toluene, acetone, and DME gave the S-polymer. Hence, in these four solvents, there appears to be no relationship between coordination abilities to zinc porphyrin and the formation of E- or S-polymers.

Solvent effect of dimer formation of monoimidazolyl-biszinc porphyrin 3Zn$_2$

3Zn$_2$ has the potential to give both E- and S-dimers, as shown in Figures 2 and S2. However, only the E-dimer was predominantly observed in the four solvents considered (toluene, acetone, $CHCl_3$, and DME), whereas **1Zn$_2$** and **2Zn$_2$** gave the S-polymer in toluene, acetone, and DME. In a previous study[23], we prepared another monoimidazolyl-biszinc porphyrin **6** linked via an ethynylene moiety, which also had the potential to give both E- and S-dimers. In the case of **6**, it gave the S-dimer even in $CHCl_3$, in the absence of pyridine, suggesting that the S-dimer is more stable than the E-dimer under pyridine-free conditions (Figure 9). In the S-dimer of biszinc porphyrin **6**, the addition of a few equivalents of pyridine induced transformation of the S-dimer to the E-dimer, coordinated by pyridine molecules (Figure S33)[23]. This result indicates that the noncoordinated zinc porphyrin linked with the imidazole moiety in the S-dimer of **6** is sensitive to solvent coordination, and the coordinated state of the zinc porphyrin destabilizes the S-dimer of **6** coordinated by coordinating molecules. Because the structures of the S-dimers of **6** and **3Zn$_2$** are similar, similar destabilization will be expected by solvent coordination to the zinc porphyrin linked with the imidazole in S-dimers of **3Zn$_2$** (Figure S34). Therefore, the stabilities of the S-dimers of **3Zn$_2$** and **3FbZn** are different, because the S-dimer of **3FbZn** has no zinc porphyrin linked with the imidazole moieties. Probably, the S-dimer of **3Zn$_2$** is destabilized, compared with that of **3FbZn**. This is a possible explanation why no S-dimer of **3Zn$_2$** was observed, although the $\Delta\Delta G^0_{298}$ values shown in Table 2 are in the range 3–9 kJ/mol. In the virtual equilibrium between the S-dimer of **3FbZn** and the E-dimer of **3Zn$_2$** (Figure S35), the energy differences are underestimated.

The difference between the two monoimidazolyl-biszinc porphyrin systems, **3Zn$_2$** and **6**, is in the connecting moieties of 1,3-butadiynylene and ethynylene, respectively[24]. The rotational barrier of the two coplanar porphyrins linked via a 1,3-butadiynylene moiety in **3Zn$_2$** is considered to be lower than in the case where linkage is via an ethynylene moiety in **6**[25]. The

distance between the two porphyrins in **3Zn₂** is greater than that in **6.**

The experimental results, specifically, that **3Zn₂** gave its E-dimer and **6** gave its S-dimer, suggest that the formation of the E-dimer of **3Zn₂** is entropy controlled, whereas the formation of the S-dimer of **6** is controlled by the larger enthalpic gain of the π–π interaction over the entropic gain of the E-dimer of **6**. In the case of the 1,3-butadiynylene systems, the enthalpic gain of the π–π interaction in S-dimer may be too small to overcome the entropic gain of the corresponding E-polymer. This albeit S-polymer of **1Zn₂** and **2Zn₂** was observed in three of the four solvents (toluene, acetone, and DME). Therefore, the inside zinc porphyrin units in the S-polymers are essential for the formation of the S-type assembly of biszinc porphyrin systems linked via a 1,3-butadiynylene moiety, which are covered by other porphyrins over both the top and the bottom.

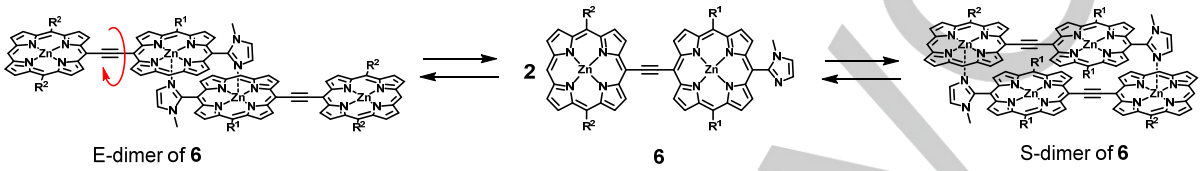

Figure 9. A structure of porphyrin derivative **6** and its self-assembled E- and S-dimers.

Comparisons of competitive dissociation constants and self-association constants among E- and S-dimers: Solvent dependency

In Table 1, competitive dissociation constants of the extended dimer of **3Zn₂** coordinated by two Im molecules (**(3Zn₂)-ExD-Im₂**), stacked dimer of **3FbZn** (**(3FbZn)-StD**), and **4Zn** dimer (**(4Zn)-D**), obtained in four solvents are compared. A smaller value indicates a larger resistance to the competitive coordination with Im, followed by the dissociation of the dimer, and hence a larger self-association property. In the case of the E-dimer of **(3Zn₂)-ExD-Im₂**, low solvent dependency was observed for K_6. Low solvent dependency was also observed for K_3 in the E-type dimer of **(4Zn)-D**, except in toluene. On the other hand, a weak solvent effect was observed for K_2 for the competitive dissociation constants of the S-dimer of **(3FbZn)-StD**. It is considered that the difference in the solvation between before and after dissociation of the S-type dimer is larger than that of the E-type dimer. In particular, a smaller K_2 value was obtained in acetone compared with the K_2 values obtained in the other solvents. This result is consistent with the fact that the competitive coordination ability of acetone toward the ZnTPP/Im complex is small, as shown in Table S1, and solvation of acetone toward the π-plane of zinc porphyrin cannot be expected to occur.

In Table 2, the self-association constants K_8, K_{10}, and K_{12} of **3Zn2-Im**, **3FbZn**, and **4Zn**, respectively, derived from the dissociation constants given in Table 1 are shown. All the values obtained in the four solvents are $>10^7$ M^{-1}, indicating that the concentrations of dissociated monomeric species are low in the absence of Im under the concentrations in the UV-vis spectra (6.0×10^{-7} M). In the cases of polymers of **1Zn₂** and **2Zn₂**, one unit of a bis(imidazolylporphyrinatozinc) molecule must make two complementary coordination bonds dissociate to afford its monomeric unit. If the two association constants are independent in a bis(imidazolylporphyrinatozinc) molecule, and the equilibrium constant $>10^7$ M^{-1}, then the probability of producing the monomer unit is too low in **1Zn₂** and **2Zn₂** under the concentration used for recording the UV–vis spectra, used as an indicator[18] (2.0×10^{-6} M) and the temperature-jump experiments (10^{-5} ~ 10^{-6} M). Therefore, a mechanism of E to S transformation via monomeric units can be eliminated. As described in the results section, no solvent-dependent structural change was observed in the dimer systems of **3Zn₂**. Therefore, the polymer system is discussed next.

Thermodynamic consideration of solvent-dependent S/E transformation

To discuss the thermodynamics of the solvent-dependent formation of E- and S-polymers, a simple model was considered (see Figure 10). Here, only an equilibrium between E-polymer and S-polymer composed of *n* numbers of **1Zn₂** is considered. We experimentally observed the existence of solvated E-polymer and/or solvated S-polymer in various solvents, as shown by equilibrium **[1]**. The positive or negative signs of $\Delta G^0_{(S/E)\ obs.}$ was determined in the experiments. For example, the sign of the $\Delta G^0_{(S/E)\ obs.}$ was positive only in $CHCl_3$; in DME it was negative. In a mixture of TCE:DME = 60:40, the $\Delta G^0_{(S/E)\ obs.}$ was nearly zero. The equilibrium **[1]** can be divided into the process of desolvation of E-polymer **[2]**, S/E transformation in vacuum **[3]**, and the solvation process of the S-polymer to give solvated S-polymer **[4]**. Thus, the thermodynamic cycle of the S/E transformation in solution is described as follows:

$\Delta G^0_{(S/E)\ obs.} = \Delta G^0_{(E)\ desolvation} + \Delta G^0_{(S/E)\ vacuum} + \Delta G^0_{(S)\ solvation}$,

where $\Delta G^0_{(E)\ desolvation}$, $\Delta G^0_{(S/E)\ vacuum}$, and $\Delta G^0_{(S)\ solvation}$ are the Gibbs free energy changes in **[2]**, **[3]**, and **[4]**, respectively. $\Delta G^0_{(S/E)\ vacuum}$ in **[3]** is constant, and it can be divided further into two terms of coordination ($\Delta G^0_{(S/E)\ coordination}$) and π–π interaction ($\Delta H^0_{(S/E)\ \pi-\pi\ interaction}$), as follows:

$\Delta G^0_{(S/E)\ vacuum} = \Delta G^0_{(S/E)\ coordination} + \Delta H^0_{(S/E)\pi-\pi\ interaction}$.

The coordination term ($\Delta G^0_{(S/E)\ coordination}$) corresponds mainly to stabilization energies of imidazole to zinc coordination (thus, the energy difference between E- and S-type coordinations), and the π–π interaction term ($\Delta H^0_{(S/E)\ \pi-\pi\ interaction}$) corresponds to the π–π interactions among the inside porphyrins in the S-polymer. The π–π interactions in the E-polymer can be considered negligible, because they are much smaller than interactions among the inside porphyrins in the S-polymer.

The sign of the coordination term, $\Delta G^0_{(S/E)\ coordination}$, is considered to be positive from the results of the dimer systems. The value of $\Delta G^0_{(S/E)\ coordination}$ per unit in the *n*-mer can be roughly estimated as being similar to the dimer system (in the order of between 10 and a dozen kJ/mol). On the other hand, to estimate the $\Delta H^0_{(S/E)\ \pi-\pi\ interaction}$ value, we tried to calculate the π–π interaction enthalpy of the inside porphyrins in the S-oligomer of **1Zn₂** without side chains. Unfortunately, calculations proved to be challenging due to the (non)availability of suitable computers and the large size of the molecular system. The free dimerization enthalpy of a zinc porphyrin derivative in a vacuum has been reported in the literature to be approximately –100 kJ/mol[26]. Although, at present, the $\Delta H^0_{(S/E)\ \pi-\pi\ interaction}$ value in a vacuum cannot be determined, the value must be negative. Furthermore, the absolute value is expected to be significantly larger than that of the $\Delta G^0_{(S/E)\ coordination}$ in a vacuum, based on the reported value of a related compound[26], and also the value ΔH = –29.2 kJ/mol obtained in the equilibrium conditions (reported earlier)[18]. Therefore, S-polymer must be more stable than E-polymer in a vacuum.

Because the coordination term is little or weakly solvent dependent, as is evident in Tables 1, 2, and S1, the π–π interaction enthalpy must be affected by solvent more sensitively. Because $\Delta G^0_{(S/E)\ vacuum}$ in **[3]** is constant, variation of the $\Delta G^0_{(S/E)\ obs.}$ in various solvents and solvent systems reflects variations in the sum of the terms of $\Delta G^0_{(E)\ desolvation}$ and $\Delta G^0_{(S)\ solvation}$ in **[2]** and **[4]**. Therefore, the present system may be referred to as a "solvation/desolvation indicator." In the case of "good solvents," such as $CHCl_3$, the $\Delta G^0_{(S/E)\ obs.}$ has a positive sign. Therefore, the sum of $\Delta G^0_{(E)\ desolvation}$ and $\Delta G^0_{(S)\ solvation}$ has a positive sign, and the absolute value is larger than that of $\Delta G^0_{(S/E)\ vacuum}$. Probably, both $\Delta G^0_{(E)\ desolvation}$ and $\Delta G^0_{(S)\ solvation}$ are positive in $CHCl_3$. Here, $\Delta G^0_{(E)\ desolvation}$ in **[2]** corresponds to solvent–solute interaction between $CHCl_3$ and zinc porphyrins in E-polymer, and the interaction stabilizes the E-polymer. The solvent–solute interaction also works between $CHCl_3$ and zinc porphyrins in the S-polymer. In this case, however, the interaction destabilizes the S-polymer. Here, we introduce the concept of a damping effect to weaken the π–π interaction in S-polymer by the solvent–solute interaction. Therefore, $\Delta G^0_{(S)\ solvation}$ in **[4]** is considered to correspond to a damping effect to weaken the π–π interaction in the S-polymer. Hence, it is clear that "good solvents" generally weaken π–π interactions. In the case of "poor solvents," such as DME, $\Delta G^0_{(S/E)\ obs.}$ has a negative sign. Therefore, the sum of $\Delta G^0_{(E)\ desolvation}$ in **[2]** and $\Delta G^0_{(S)\ solvation}$ in **[4]** is negative, or, if positive, the absolute value of that must be smaller than that of $\Delta G^0_{(S/E)\ vacuum}$. In these cases, the solvation ability for E-polymer as well as a damping effect to weaken the π–π interaction in S-polymer is lower than in the case of "good" solvents. There may also be strong solvent–solvent interaction, with an associated solvophobic effect.

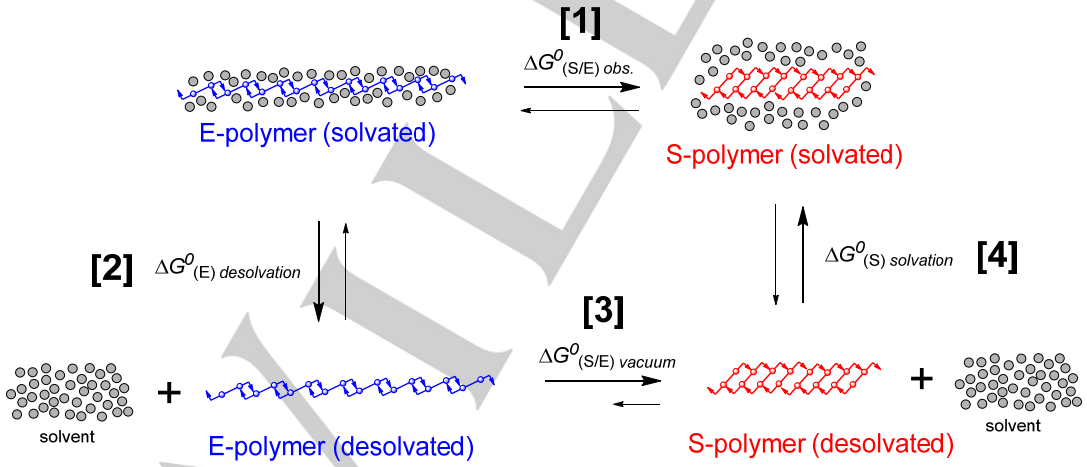

Figure 10. A thermodynamic cycle of solvent-dependent transformation from E-polymer to S-polymer. **[1]** = **[2]**+**[3]**+**[4]**

The process of S/E transformation

The results of the GPC data of **1Zn₂** and **2Zn₂** obtained, using solvent mixtures with various ratios of $CHCl_3$:DME content, revealed changes in the lengths of E-polymers. Thus, the lengths of relatively shorter E-polymers in 100% $CHCl_3$ were extended in $CHCl_3$:DME = 90:10, whereafter they became

increasingly shorter as the DME content increased. Instead of E-polymers, S-polymers were now observed to be long; they reached the exclusion limit in $CHCl_3$:DME = 70:30 and 60:40. Because the latter shortening process of E-polymers is accompanied by the formation of S-polymers, the phenomenon is considered to be the transformation to S-polymer from E-polymer (hereafter referred to as S/E transformation).

A mechanism via monomeric units can be eliminated in the S/E transformation because self-association constants of both E- and S-type dimers are $>10^7$ M^{-1}, and the probability of dissociation of the two complementary coordination bonds to afford the monomer unit is too low in **1Zn₂** and **2Zn₂**. Therefore, phenomena involving the monomer unit of **1Zn₂** and **2Zn₂** as shown in Eq 14 hardly occur under equilibrium conditions. Instead of a mechanism via monomeric units, an exchange mechanism among E- and S-polymers is plausible. Possible dynamic phenomena in the S/E transformation are shown as Eq 16–22 in Figures 11 and 12. In the exchange mechanism, some equilibrium constants must vary, depending on solvents or solvent compositions. GPC experiments, when the DME content is increased, the association constant between S-polymers, K_{22}, will increase gradually, in comparison with that between E-polymers, K_{16}. (Eq 22 and 16, respectively). This solvent effect mainly occurs inside parts of the S- and E-polymers. However, the effect is relatively small for the association constant with **4Zn** at the terminal ends of end-capped E-polymer, K_{15}, as well as that of dimer formation of **4Zn**, K_{13} (Eq 15 and 13, respectively). In the S/E transformation in the temperature-jump experiments, transformation to S-polymer is accelerated after formation of the nucleus of S-polymer. The S-dimer of **3Zn₂** was never been observed instead of the E-dimer, even in DME.

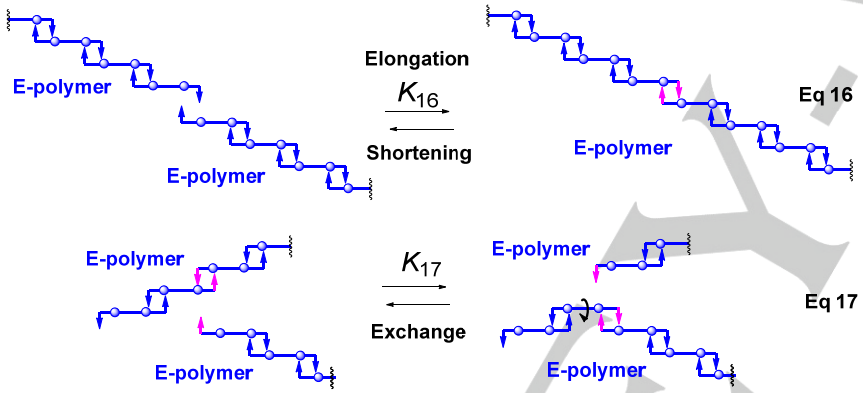

Figure 11. Possible self-assembly patterns between E-polymers of **1Zn₂**.

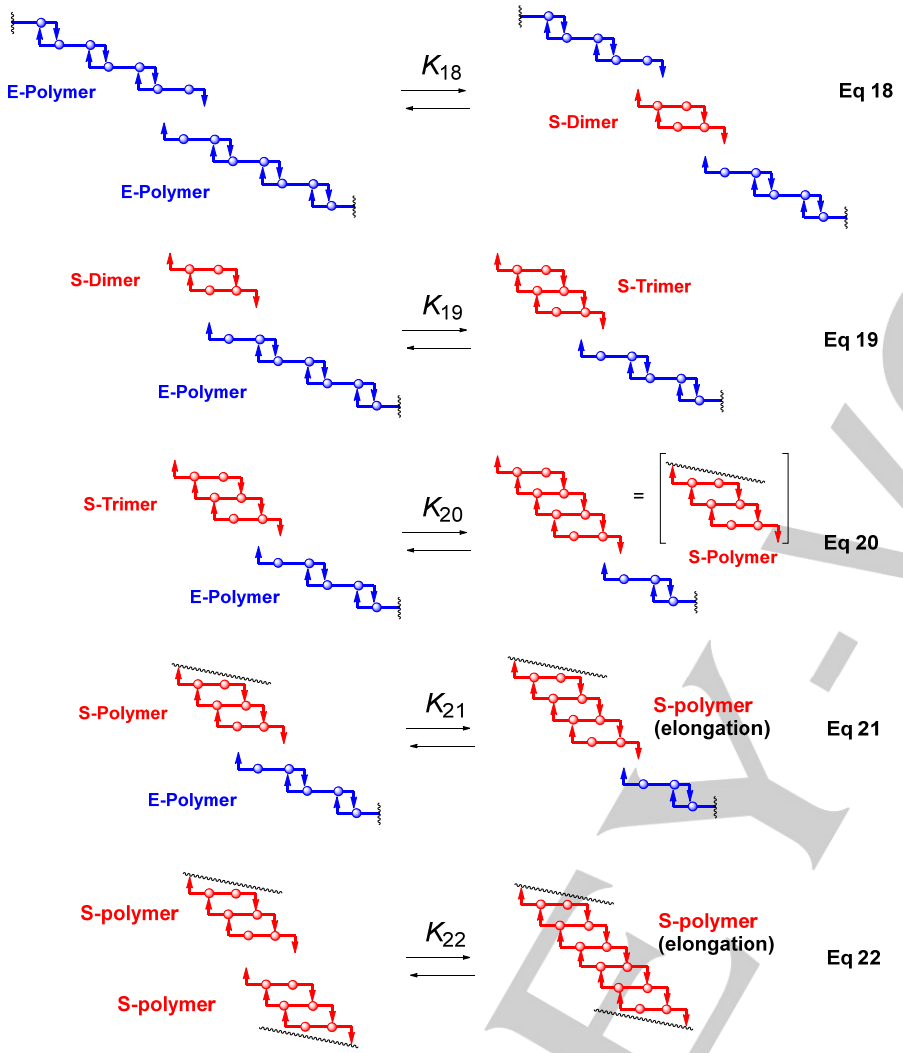

Figure 12. Possible self-assembly patterns among E-polymers and S-oligomers of **1Zn₂**.

These results indicated that the formation of S-dimer and S-trimer of **1Zn₂** and **2Zn₂** in Eq 18 and 19 rarely occurs; the equilibria are shifted toward the formation of E-polymer. However, when nuclei of S-polymers are formed, the following elongation proceeds smoothly, as shown in Eq 20–22. The order of the transformation from E- to S-polymer was determined as 2.3 from the kinetics. This value is consistent with the exchange mechanism, and suggests that it is possible to extend both terminals of the nuclei of S-polymers.

In the exchange mechanisms, capping the active terminals in E-polymers is expected to affect the equilibria significantly. In fact, **1Zn₂** end-capped by **4Zn** affected the distribution of the length of E-polymers in GPC experiments, and also partially suppressed the transformation to S-polymers, even at high DME compositions.

The proposed exchange mechanism is summarized in Figure 13. When the DME composition increases, a long E-polymer **A** is partially dissociated to form two shorter E-polymers (**B**). The two active terminals interact with each other to give S-dimer and two excluded E-polymers (**C**). Although the S-dimer is less stable, it sometimes gives S-trimer, followed by an S-*n*-mer (**D**). Successive elongation occurs from the S-*n*-mer, as a seed, to give S-polymer (**E**).

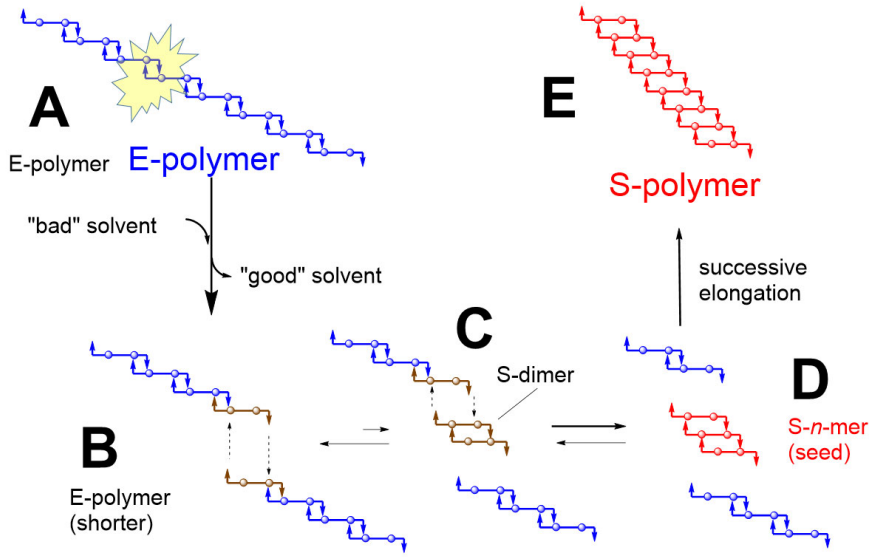

Figure 13. A proposed exchange mechanism of transformation from imidazole end-capped E-polymer into S-polymer. Dissociation of imidazole to zinc bonds occurs at an inside of the polymer to give end-cap free imidazolyl zinc porphyrin moieties at the terminals as **A**. When complementary coordination occurs as **B**, an S-dimer is produced transiently as **C**. S-dimer is probably more unstable than E-type structures, but it sometimes grows into S-*n*-mer as **D**, which becomes a seed of S-polymer. Successive elongation from S-*n*-mer gives extremely long polymer.

Transition among E-polymers

In the GPC experiments, the length of E-polymers was relatively short in the case of 100% $CHCl_3$ solvent, whereas in $CHCl_3$:DME = 90:10 the length was extended to the maximum (Figures 5 and S22). On the other hand, the association constants of ZnTPP and Im decreased when the DME content in $CHCl_3$ was increased (see in Table S1). The decrease in association constants will result in rather short E-polymers. Therefore, the observed extension of E-polymer cannot be explained from changes of association constants alone. The unique phenomenon is now discussed.

When we consider only the porphyrin skeleton, the extension of E-polymer is entropically unfavorable because the degree of freedom of the E-polymer decreases. Enthalpic compensation by the coordination bond is not expected for the entropic loss because the association constant decreases in the solvent mixture $CHCl_3$:DME = 90:10 (compared with 100:0). Solvation between the porphyrin skeleton and DME is not expected to take place because DME is a “poor” solvent. Therefore, the unique extension phenomenon cannot be explained from the thermodynamics of only the porphyrin skeleton. The thermodynamics including solvent molecules must be considered. Unfortunately, it is rather difficult to observe solvent molecules that have interacted with the porphyrin, because the interaction is very weak, and the solvent molecules exchange rapidly with other solvent molecules. Nonetheless, we would like to discuss the unique phenomenon in more detail.

The equilibrium among the short and long E-polymers must follow the second law of thermodynamics. In the thermodynamics of only the porphyrin skeleton, neither enthalpic nor entropic gains are expected to shift the equilibrium to long E-polmer. Since the extension phenomenon occurs in the presence of only small amounts of DME, it is considered to be related to entropy gain of the minor solvent, DME. Entropy-driven supramolecular formation by desolvation of solvent molecules restricted is sometimes observed between macrocycles and ligands[27], especially in water[28]. The extension phenomenon occurred in the cases of both **1Zn$_2$** and **2Zn$_2$**, as shown in Figures 5 and S22, indicating that it does not depend on the substituent groups on the porphyrin skeleton. Based on this, therefore, selective solvation of DME molecules towards the terminal imidazolyl moieties followed by desolvation is one possible explanation of the supramolecular formation driven by entropy gain of solvent molecules.

An equilibrium model is proposed as shown in Figure 14. In equilibrium (1), the formation of two short E-polymers is dominant in 100% $CHCl_3$, due to entropy control, in which the formation of a large number of the short E-polymers is favorable. In the presence of small amounts of DME, the DME molecules may solvate the terminal imidazolyl moieties selectively, as shown in equilibrium (2). Because the noncoordinating imidazolyl moieties have a polar unshared electron pair, they may prefer to be solvated by polar DME molecules. The formation of longer E-polymers can release the solvated DME molecules to the system, which is entropically favorable for the total system. This is speculation; however, it can be affirmed that thermodynamics of the minor solvent, DME, controls the equilibrium.

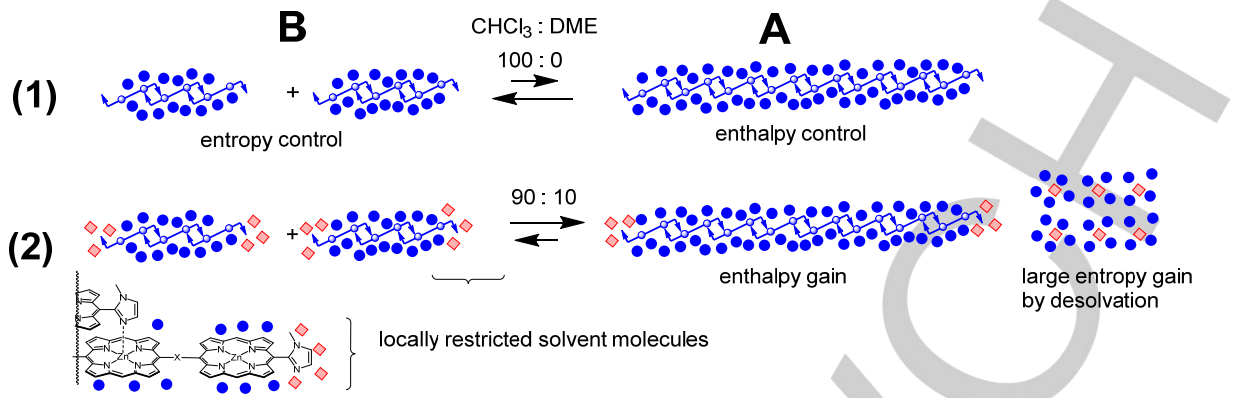

Figure 14. Proposed equilibriums of E-polymers. Both short and long E-polymers are stabilized by $CHCl_3$, (as illustrated by blue filled circles) and the contributions per E-polymer unit are comparable. In 100% $CHCl_3$, formation of short E-polymers is entropically favorable, whereas formation of long E-polymers is enthalpically favorable. An equilibrium mixture is obtained on the balance. In the presence of polar DME molecules (as pink diamonds), they are expected to solvate polar imidazolyl moieties of E-polymers existing at the terminals. Since the DME molecules are localized at the terminals, their motions may be restricted. When long E-polymer is formed, the restricted DME molecules are released, and large entropy gain is expected as well as enthalpy gain by forming complementary coordination.

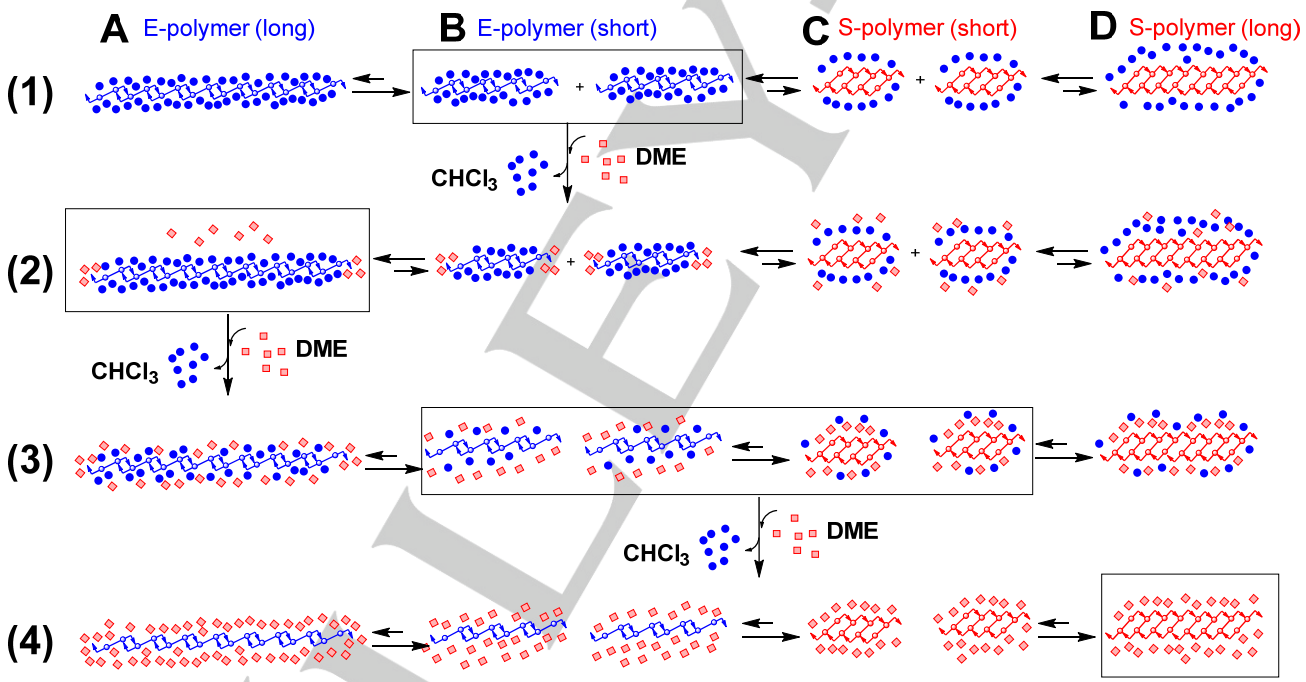

Figure 15. Schematic images of DME-induced transformation from E-polymer into S-polymer. For simplifying, only four states (A: long E-polymer; B: short E-polymers; C: short S-polymers; D: long S-polymer) are considered. (**1**) In 100% chloroform solution, equilibrium among E-polymers gives short E-polymers. (**2**) Small amounts of DME shift the equilibrium to long E-polymer side as discussed in Figure 14. (**3**) By further addition of DME, the long E-polymers are destabilized due to the partial removal of chloroform solvent to give short E-polymers. The short E-polymers produce S-dimers and S-*n*-mer, which become seeds for S-polymers as shown in Figure 13. On the balance point, a mixture of E- and S-polymers is observed, and it was used for temperature-jump experiments as shown in Figure 8. (**4**) When contents of chloroform become minor, S-polymers are stabilized by self-association as well as solvophobic effect. S-polymers are dominant by exclusion of E-polymers.

Summary of successive transformation processes

Finally, the proposed mechanism for transition of short E- to long E-polymers followed by S/E transformation involving solvent molecules is illustrated in Figure 15. To simplify the successive processes, equilibria among only four states are considered here: a long E-polymer **A**, two short E-polymers **B**, two short S-polymers **C**, and a long S-polymer **D**. (Filled circles and pink diamonds indicate $CHCl_3$ and DME molecules, respectively.

Major components are shown within rectangles.) (1) In 100% $CHCl_3$, **B** is dominant. (2) In the presence of small amounts of DME, **A** becomes dominant. (3) Increasing the DME composition causes **A** to destabilize, to give a mixture of **B** and **C**. (4) In the absence of $CHCl_3$, neither stabilization of E-polymer nor a damping effect to weaken the π–π interaction in S-polymer is expected; as a result, **D** becomes dominant.

What is different between the present system and most of the solvent-dependent supramolecular polymers in which monomer/polymer transition occurs? In the latter systems, observation of supramolecular polymers is significantly concentration dependent[29] and/or temperature dependent[20b, 30]. Under dilute conditions, polymerization occurs only in a few solvents and solvent systems, usually either highly hydrophilic or hydrophobic. On the other hand, the present system is supported by not only strong but also labile coordination bonds. On the basis of the characteristic coordination motif, the system is designed to give two types of coordination polymers, affected by the solvent used. As a result, compounds **1Zn₂** and **2Zn₂** always give the two types of coordination polymers exclusively, without proceeding via the monomers, in most solvents and liquids, even under highly diluted conditions. These unique features make it possible to determine the solvent dependency among various solvents under the same concentration and temperature conditions. This is significantly advantageous. Therefore, the collected data can be directly compared among different solvents and porphyrin derivatives. Indications are, therefore, that the system could become a versatile chemical indicator to detect van der Waals interactions among solvents and solutes.

Conclusions

Significant aspects of the thermodynamics and the mechanism were unveiled for the solvent-dependent formation of E- or S-polymers as well as the transformation from E- to S-polymers composed of **1Zn₂** or **2Zn₂**.

The contributions of both the E- and S-type complementary coordination and the π–π interaction in E- and S-polymers were considered separately by comparing E- and S-dimer models. The results indicated that the coordination terms were weakly or little solvent dependent, and that both the E- and S-type complementary coordination interactions were very strong. This, then, suggested that the transformation from E- to S-polymers occurs via an exchange mechanism among the polymers, not via monomers. However, π–π interaction works effectively only with the inside porphyrins in an S-polymer and is strongly solvent dependent. The formation of E- or S-polymers in solution is determined by total energies and the type of solvent used (Figure 10). Because the Gibbs free energy change from E-polymer to S-polymer in vacuum ($\Delta G^0_{(S/E)\ vacuum}$) is constant, and probably significantly negative, the solvent dependency in the formation of E- or S-polymer depends on the sum of the Gibbs free energy changes of desolvation of E-polymer ($\Delta G^0_{(E)\ desolvation}$) and solvation of S-polymer ($\Delta G^0_{(S)\ solvation}$), which works as a damping effect to weaken the π–π interaction in S-polymers in solution. For example, in a "good" solvent, such as $CHCl_3$ and TCE, both $\Delta G^0_{(E)\ desolvation}$ and $\Delta G^0_{(S)\ solvation}$ are considered to be positive, and the sum of the energies must overcome the $\Delta G^0_{(S/E)\ vacuum}$. In this case, solvated S-polymer is destabilized by "good" solvent, to give desolvated S-polymer in equilibrium **[4]** in Figure 10. Although the desolvated S-polymer is more stable than the desolvated E-polymer in vacuum **[3]**, the E-polymer is stabilized by "good" solvent to give solvated E-polymer in **[2]**. Therefore, the formation of E-polymer in "good" solvent can be explained. Here, $\Delta G^0_{(E)\ desolvation}$ corresponds to solvent–solute interaction between "good" solvent molecules and zinc porphyrins in E-polymer, whereas $\Delta G^0_{(S)\ solvation}$ corresponds to a damping effect to weaken the π–π interaction in S-polymer in solution. The present system actually monitors solvation and desolvation behaviors—it may, therefore, be referred to as a "solvation/desolvation indicator."

The transformation from E- to S-polymers was also monitored by GPC. Polymer lengths of E-polymers were varied. Although no monomer or dimer species was observed in GPC analysis, it became clear, based on the end-capping experiments, that the terminal imidazolylporphyrinatozinc moieties on E-polymer are important in the transformation of E- to S-polymer. The order of the transformation from E- to S-polymer was determined as 2.3, which supports the exchange mechanism among the polymers.

The formation of E- or S-polymer is fully exclusive of each other in one self-assembled polymer chain. This is because the zinc porphyrin moieties take only the five-coordinate state in solution. (In a special case, the six-coordinate state of a zinc porphyrin moiety was observed in solution[31].) Because the number of components in both E- and S-polymers is very high (>20 000), the system has a highly positive allosteric effect. During the change in polymer lengths and transformation from E- to S-polymer, UV–vis spectra of long and short E-polymers are identical, as well as those among all S-polymers. The above facts now facilitate simplification of the complicated phenomena observed in GPC experiments as an apparent two-state change in the UV–vis spectra. These features are advantageous in terms of now being able to use the system as a chemical indicator to detect van der Waals interactions very easily and sensitively, using a conventional UV–vis spectrometer.

Experimental Section

General Procedure. All chemicals and solvents were of commercial reagent quality and used without further purification unless otherwise stated. $CHCl_3$ (Kanto, extra pure) stabilized with 0.5–1% ethanol was used. UV-vis absorption spectra were collected on JASCO V-660 spectrometer at 298 K.

Materials. Tetraphenylporphyrinatozinc (ZnTPP) was prepared by referring to the reported procedure[32]. Preparations of bis(imidazolylporphyrinatozinc), **1Zn₂** and **2Zn₂**, monoimidazolylbisporphyrin derivatives, **3Zn₂** and **3FbZn**, and monoimidazolylporphyrinatozinc **4Zn** are reported previously.[18]

UV-vis titration. To a 6.0×10^{-7} M solution of ZnTPP in various solvents (acetone, DME, and chloroform) or mixtures of chloroform and DME (90:10, 80:20, and 70:30), corresponding solution of Im was added. The UV-vis spectra were recorded. (Figures S4~S9) The spectral changes were plotted as a function of added Im, and the association constant, K_{S1}, was determined by curve fitting analysis as formation of 1:1 complex as shown in Eq S1. The association constants in various solvents are tabulated in Table S1. The association constants in toluene was referred to a literature[33].

To a 6.0×10^{-7} M solution of **3Zn$_2$**, **3FbZn**, and **4Zn** in four solvents (acetone, DME, toluene, and chloroform), the corresponding solution of Im was added. The UV-vis spectra were recorded. (Figures S10~S21) The spectral changes were plotted as a function of the added Im as shown in the inset. The dissociation process of **(3Zn$_2$)-ExD** into **3Zn$_2$-Im$_2$** (Eq 1) includes Eq 4-6 in Figure 3. To compare the dissociation constants among **3Zn$_2$**, **3FbZn**, and **4Zn** with a same dimension, the competitive dissociation constants, K_2, K_3, and K_6 were determined as described in the text. The dissociation constants are tabulated in Table 1.

GPC analyses. Analytical GPC were carried out on a JASCO PU-2080plus and MD-2018plus system equipped with a PLgel 20μm MIXED-A 300×7.5 mm column (Polymer Laboratory, polystyrene-based, Exclusion limit 40,000 kDa). A sample of **1Zn$_2$** or **2Zn$_2$** was dissolved in chloroform to adjust into ca. 6×10^{-4} M, and 10 μL of the solution was injected through a Rheodyne® injection valve for HPLC, followed by mixing with various eluents of mixtures of $CHCl_3$ and 1,2-dimethoxyethane (DME) in a stainless tube. The mixture was subsequently introduced into the GPC column. Their transformed structures and the distributions of sizes are estimated from their retention times (RT) and UV-vis absorption spectra recorded on a photodiode-array (PDA) detector. Mixtures of $CHCl_3$ (extra grade) and DME (extra grade) (100:0 ~ 60:40) were used as eluents. Flow rate of 1mL/min was used. Since the distribution and the composition of E- and S-polymers obtained the flow rate (1.0 mL/min) were very close to those obtained in flow rate of 0.5 mL/min (Figures S33 and 34), the compositions and lengths of supramolecular polymers observed under the conditions are considered to be thermodynamic products under the solvent composition. Calibration plots were prepared by using standard polystyrenes (16,100 kDa, 1,860 kDa, 70 kDa, supplied from Tosoh) and a porphyrin derivative **5** (in Figure S35, 1.162 kDa) [34].

End-capped **1Zn$_2$** were prepared by mixing appropriate ratios of **4Zn** and, **1Zn$_2$** in pyridine. Each mixture was concentrated under reduced pressure, and the residues were dissolved in $CHCl_3$ to adjust the concentrations of **1Zn$_2$** into ca. 3×10^{-4} M. 10 μL of the solution was injected.

Kinetics by temperature-jump experiments. Concentration-dependency of transformation of E-polymer into S-polymer was examined. Samples of appropriate concentration (15, 11, 10, 7.0, and 3.8×10^{-6} M) of **2Zn$_2$** in a mixture of TCE and DME (60/40 vol/vol) were prepared. In the binary solvent system, E-polymer and S-polymer of **2Zn$_2$** coexisted, and they were in equilibrium. A sample were set in a UV-vis cell with a Teflon cap, and the sample was heated into 70°C in a UV-vis apparatus with Peltier temperature variable system. At 70°C, E-polymer of **2Zn$_2$** was observed almost completely. Then, temperature of the sample was set at 20°C, and the absorbance change at 768 nm was recorded.

Keywords: van der Waals interaction • π–π interaction • allosteric effect • gel permeation chromatography (GPC) • supramolecular polymer

[1] Y. Hong, J. W. Y. Lam, B. Z. Tang, *Chem. Commun.* **2009**, 4332-4353.
[2] a) C. H. Alarcón, S. Pennadam, C. Alexander, *Chem. Soc. Rev.* **2005**, *34*, 276-285; b) X. Yan, F. Wang, B. Zheng, F. Huang, *Chem. Soc. Rev.* **2012**, *41*, 6042-6065; c) Z. Qi, C. A. Schalley, *Acc. Chem. Res.* **2014**, *47*, 2222-2233; d) A. J. McConnell, C. S. Wood, P. P. Neelakandan, J. R. Nitschke, *Chem. Rev.* **2015**, *115*, 7729-7793; e) T. Haino, *The Chemical Record* **2015**, *15*, 837-853; f) Y. F. Han, Y. K. Tian, Z. J. Li, F. Wang, *Chem. Soc. Rev.* **2018**, *47*, 5165-5176.
[3] B. L. Feringa, R. A. van Delden, N. Koumura, E. M. Geertsema, *Chem. Rev.* **2000**, *100*, 1789-1816.
[4] a) Y. Kubo, S. y. Maeda, S. Tokita, M. Kubo, *Nature* **1996**, *382*, 522-524; b) A. P. de Silva, H. Q. N. Gunaratne, T. Gunnlaugsson, A. J. M. Huxley, C. P. McCoy, J. T. Rademacher, T. E. Rice, *Chem. Rev.* **1997**, *97*, 1515-1566; c) X. Peng, Z. Yang, J. Wang, J. Fan, Y. He, F. Song, B. Wang, S. Sun, J. Qu, J. Qi, M. Yan, *J. Am. Chem. Soc.* **2011**, *133*, 6626-6635; d) G. Fukuhara, *Journal of Inclusion Phenomena and Macrocyclic Chemistry* **2019**, *93*, 127-143; e) L. You, D. Zha, E. V. Anslyn, *Chem. Rev.* **2015**, *115*, 7840-7892.
[5] a) L. Brunsveld, B. J. B. Folmer, E. W. Meijer, R. P. Sijbesma, *Chem. Rev.* **2001**, *101*, 4071-4097; b) L.-J. Chen, H.-B. Yang, *Acc. Chem. Res.* **2018**, *51*, 2699-2710.
[6] a) J. L. Fan, M. M. Hu, P. Zhan, X. J. Peng, *Chem. Soc. Rev.* **2013**, *42*, 29-43; b) J. S. Wu, W. M. Liu, J. C. Ge, H. Y. Zhang, P. F. Wang, *Chem. Soc. Rev.* **2011**, *40*, 3483-3495.
[7] E. Yashima, N. Ousaka, D. Taura, K. Shimomura, T. Ikai, K. Maeda, *Chem. Rev.* **2016**, *116*, 13752-13990.
[8] W. B. Jennings, B. M. Farrell, J. F. Malone, *Acc. Chem. Res.* **2001**, *34*, 885-894.
[9] E. A. Meyer, R. K. Castellano, F. Diederich, *Angew. Chem. Int. Ed.* **2003**, *42*, 1210-1250.
[10] B. P. Abbott, R. Abbott, T. D. Abbott, M. R. Abernathy, F. Acernese, K. Ackley, C. Adams, T. Adams, P. Addesso, R. X. Adhikari, V. B. Adya, C. Affeldt, M. Agathos, K. Agatsuma, N. Aggarwal, O. D. Aguiar, L. Aiello, A. Ain, P. Ajith, B. Allen, A. Allocca, P. A. Altin, S. B. Anderson, W. G. Anderson, K. Arai, M. A. Arain, M. C. Araya, C. C. Arceneaux, J. S. Areeda, N. Arnaud, K. G. Arun, S. Ascenzi, G. Ashton, M. Ast, S. M. Aston, P. Astone, P. Aufmuth, C. Aulbert, S. Babak, P. Bacon, M. K. M. Bader, P. T. Baker, F. Baldaccini, G. Ballardin, S. W. Ballmer, J. C. Barayoga, S. E. Barclay, B. C. Barish, D. Barker, F. Barone, B. Barr, L. Barsotti, M. Barsuglia, D. Barta, J. Bartlett, M. A. Barton, I. Bartos, R. Bassiri, A. Basti, J. C. Batch, C. Baune, V. Bavigadda, M. Bazzan, B. Behnke, M. Bejger, C. Belczynski, A. S. Bell, C. J. Bell, B. K. Berger, J. Bergman, G. Bergmann, C. P. L. Berry, D. Bersanetti, A. Bertolini, J. Betzwieser, S. Bhagwat, R. Bhandare, I. A. Bilenko, G. Billingsley, J. Birch, R. Birney, O. Birnholtz, S. Biscans, A. Bisht, M. Bitossi, C. Biwer, M. A. Bizouard, J. K. Blackburn, C. D. Blair, D. G. Blair, R. M. Blair, S. Bloemen, O. Bock, T. P. Bodiya, M. Boer, G. Bogaert, C. Bogan, A. Bohe, et al. (LIGO Scientific Collaboration and Virgo Collaboration) *Phys. Rev. Lett.* **2016**, *116*, 061102.
[11] D. Castelvecchi, in *Nature News*, Springer Nature, **Oct 3, 2017**.
[12] J. w. Hwang, P. Li, K. D. Shimizu, *Org. Biomol. Chem.* **2017**, *15*, 1554-1564.
[13] a) C. A. Hunter, M. C. Misuraca, S. M. Turega, *Chem. Sci.* **2012**, *3*, 2462-2469; b) S. Henkel, M. C. Misuraca, Y. Ding, M. Guitet, C. A. Hunter, *J. Am. Chem. Soc.* **2017**, *139*, 6675-6681.
[14] L. Yang, C. Adam, G. S. Nichol, S. L. Cockroft, *Nat. Chem.* **2013**, *5*, 1006.
[15] W. R. Carroll, C. Zhao, M. D. Smith, P. J. Pellechia, K. D. Shimizu, *Org. Lett.* **2011**, *13*, 4320-4323.
[16] a) S. Shinkai, M. Ikeda, A. Sugasaki, M. Takeuchi, *Acc. Chem. Res.* **2001**, *34*, 494-503; b) C. A. Hunter, H. L. Anderson, *Angew. Chem. Int. Ed.* **2009**, *48*, 7488-7499.
[17] L. Ding, Y. Bai, Y. Cao, G. Ren, G. J. Blanchard, Y. Fang, *Langmuir* **2014**, *30*, 7645-7653.

[18] A. Satake, Y. Suzuki, M. Sugimoto, T. Shimazaki, H. Ishii, Y. Kuramochi, *Chem. Eur. J.* **2018**, *24*, 14733-14741.

[19] P. Jonkheijm, P. van der Schoot, A. P. H. J. Schenning, E. W. Meijer, *Science* **2006**, *313*, 80-83.

[20] a) P. A. Korevaar, S. J. George, A. J. Markvoort, M. M. J. Smulders, P. A. J. Hilbers, A. P. H. J. Schenning, T. F. A. De Greef, E. W. Meijer, *Nature* **2012**, *481*, 492; b) S. Ogi, K. Sugiyasu, S. Manna, S. Samitsu, M. Takeuchi, *Nat. Chem.* **2014**, *6*, 188-195.

[21] V. Gutmann, *Electrochim. Acta* **1976**, *21*, 661-670.

[22] A. Satake, Y. Kobuke, *Tetrahedron* **2005**, *61*, 13-41.

[23] A. Satake, J. Tanihara, Y. Kobuke, *Inorg. Chem.* **2007**, *46*, 9700-9707.

[24] a) P. P. Ghoroghchian, P. R. Frail, K. Susumu, T.-H. Park, S. P. Wu, H. T. Uyeda, D. A. Hammer, M. J. Therien, *J. Am. Chem. Soc.* **2005**, *127*, 15388-15390; b) M. Morisue, I. Ueno, *J. Phys. Chem. B* **2018**, *122*, 5251-5259.

[25] M. U. Winters, J. Kärnbratt, M. Eng, C. J. Wilson, H. L. Anderson, B. Albinsson, *J. Phys. Chem. C* **2007**, *111*, 7192-7199.

[26] S. Ehrlich, J. Moellmann, S. Grimme, *Acc. Chem. Res.* **2013**, *46*, 916-926.

[27] D. J. Cram, H. J. Choi, J. A. Bryant, C. B. Knobler, *J. Am. Chem. Soc.* **1992**, *114*, 7748-7765.

[28] a) Y. Inoue, T. Hakushi, Y. Liu, L. H. Tong, B. J. Shen, D. S. Jin, *J. Am. Chem. Soc.* **1993**, *115*, 475-481; b) M. V. Rekharsky, Y. Inoue, *Chem. Rev.* **1998**, *98*, 1875-1917; c) E. A. Meyer, R. K. Castellano, F. Diederich, *Angew. Chem. Int. Ed.* **2003**, *42*, 1210-1250; (d) K. N. Houk, A. G. Leach, S. P. Kim, X. Zhang, *Angew. Chem. Int. Ed.* **2003**, *42*, 4872-4897.

[29] a) T. F. A. De Greef, M. M. J. Smulders, M. Wolffs, A. P. H. J. Schenning, R. P. Sijbesma, E. W. Meijer, *Chem. Rev.* **2009**, *109*, 5687-5754; b) Z. Chen, A. Lohr, C. R. Saha-Moller, F. Würthner, *Chem. Soc. Rev.* **2009**, *38*, 564-584; c) J. A. Wytko, C. Kahlfuss, Y. Kikkawa, J. Weiss, *Helv. Chim. Acta* **2019**.

[30] T. Fukui, N. Sasaki, M. Takeuchi, K. Sugiyasu, *Chem. Sci.* **2019**, *10*, 6770-6776.

[31] L. Favereau, A. Cnossen, J. B. Kelber, J. Q. Gong, R. M. Oetterli, J. Cremers, L. M. Herz, H. L. Anderson, *J. Am. Chem. Soc.* **2015**, *137*, 14256-14259.

[32] A. D. Adler, F. R. Longo, J. D. Finarelli, J. Goldmacher, J. Assour, L. Korsakoff, *J. Org. Chem.* **1967**, *32*, 476-476.

[33] W. A. Kaplan, R. A. Scott, K. S. Suslick, *J. Am. Chem. Soc.* **1990**, *112*, 1283-1285.

[34] K. Yoneyama, R. Suzuki, Y. Kuramochi, A. Satake, *Molecules* **2019**, *24*, 2166.

Entry for the Table of Contents (Please choose one layout)

FULL PAPER

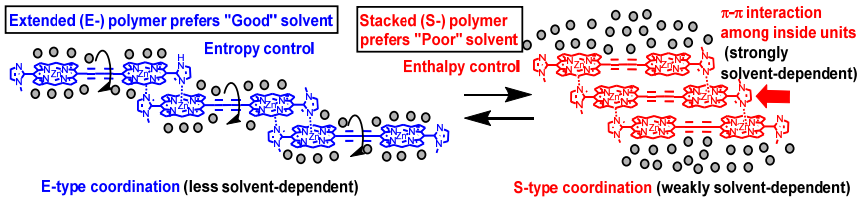

Significant aspects of the thermodynamics and the mechanism were unveiled for the solvent-dependent formation of E- or S-polymers as well as the transformation from E- to S-polymers composed of bis(imidazolylporphyrinatozinc) molecules.

Akiharu Satake, Yuki Suzuki, Motonobu Sugimoto, Yusuke Kuramochi*

Page No. – Page No.

Mechanistic Study of Solvent-Dependent Formation of Extended and Stacked Supramolecular Polymers Composed of Bis(imidazolylporphyrinatozinc) Molecules